Supplemental information for: "Brillouin laser-driven terahertz oscillator up to 3 THz with femtosecond-level timing jitter"

Brendan Heffernan[1*], James Greenberg[1], Takashi Hori[2], Tatsuya Tanigawa[2], Antoine Rolland[1]

[1]Boulder Research Labs, IMRA, America Inc., 1551 S. Sunset Street, Longmont, 80501, CO, USA.
[2]Japan Branch Office, IMRA, America Inc., 2-1 Asahi-machi, Aichi, Japan.

*Corresponding author(s). E-mail(s): bheffern@imra.com;
Contributing authors: jgreenbe@imra.com; arolland@imra.com;

Opto-THz waves

Here we provide a derivation of THz phase noise when produced through photomixing as well as provide mathematical formalism for the concept of opto-THz waves. In classical electromagnetism, light is characterized by its electric field vector E. The orientation of this vector determines the direction of light polarization [1]. Because electromagnetic waves are transverse, the electric fields E_1 and E_2 of monochromatic plane waves can be described as:

$$E_{1,2}\cos(\omega_{1,2}t - k_{1,2}z). \tag{1}$$

Let k denote the wave vector, which, for simplicity, is aligned along the z-axis. We drop this spatial dependence to focus more clearly on the frequency and phase components. The electric field of the total opto-THz wave can be expressed as:

$$E(t) = E_1\cos(\omega_1 t - \phi_1) + E_2\cos(\omega_2 t - \phi_2), \tag{2}$$

where E_1, E_2 are the constant amplitudes of the two optical lines. The phase of each field is considered to be a constant, time-averaged value with time-dependent fluctuations about the mean such that $\phi_{1,2} = \Phi_{1,2} + \varphi_{1,2}(t)$, where Φ_1 and Φ_2 are constants.

Derived from equ. 2, the Poynting vector Π of such optical electric field is written as follows:

$$\Pi(t) \propto \mid E(t) \mid^2 = E_1^2 \cos^2(\omega_1 t - \phi_1) + E_2^2 \cos^2(\omega_2 t - \phi_2) + 2E_1 E_2 \cos(\omega_1 t - \phi_1) \cos(\omega_2 t - \phi_2) \quad (3)$$

Equation 3 can be rewritten as:

$$\begin{aligned} \Pi(t) &\propto \mid E(t) \mid^2 \\ &= \frac{E_1^2}{2}[1 + \cos(2\omega_1 t - 2\phi_1)] \\ &\quad + \frac{E_2^2}{2}[1 + \cos(2\omega_2 t - 2\phi_2)] \\ &\quad + E_1 E_2[\cos((\omega_1 - \omega_2)t - (\phi_1 - \phi_2)) \\ &\qquad + \cos((\omega_1 + \omega_2)t - (\phi_1 + \phi_2))]. \end{aligned} \quad (4)$$

The Poynting vector, as described in equ. 4 has a slow component with an angular frequency of $\omega_1 - \omega_2$ and a phase of $\phi_1 - \phi_2$. It is this component that is responsible for optically carrying the THz wave. To convert an opto-THz wave to THz radiation, the two electric fields that make up the opto-THz wave are mixed on a photodiode. Uni-traveling-carrier photodiodes (UTC-PD's) provide effective conversion. Using UTC-PD's, radiation up to 3 THz have been observed [2]. The average optical power P_{opt} over the photodiode time constant τ_{PD} ($\mid \omega_1 - \omega_2 \mid \ll 1/\tau_{PD} \ll \omega_1, \omega_2$) is:

$$P_{opt}(t) \propto E_1^2 + E_2^2 + 2E_1 E_2 \cos((\omega_1 - \omega_2)t - (\phi_1 - \phi_2)) \quad (5)$$

The photocurrent I_s through the photodiode load R_{load} can be expressed as:

$$I_s(t) = \eta E(t) \quad (6)$$

with η, the photodiode responsivity. The emitted terahertz power P_{THz} through this photodetection process can be written as follows:

$$P_{THz} = \langle R_{load} \times I_s^2(t) \rangle \propto R_{load} \times P_{opt}(t) \quad (7)$$

The phase of the opto-THz wave is $\phi_1 - \phi_2$. As such, the phase fluctuations of the opto-THz φ_{THz} will be dominated by the phase fluctuations φ_1 and φ_2 of the two optical lines as:

$$\varphi_{THz}(t) = \varphi_1(t) - \varphi_2(t). \quad (8)$$

When phase fluctuations $\varphi_1(t)$ and $\varphi_2(t)$ are strongly correlated, it can significantly reduce the opto-THz wave phase fluctuations, as these correlated fluctuations cancel upon photomixing. However, photomixing introduces its own phase noise [3]. This includes flicker noise $\varphi_{1/f}$, referred to as 1/f noise, as well as thermal and shot white phase noise φ_{TandS}. Finally, we can write the terahertz signal as such:

$$E_{THz}(t) = V_{THz}[1 + \alpha_{THz}(t)] \cos[\omega_{THz} * t + \varphi_{THz}(t) + \varphi_{1/f} + \varphi_{TandS}] \quad (9)$$

where V_{THz} is the time-averaged field amplitude and $\alpha_{THz}(t)$ is the time-dependent fluctuation of the amplitude, which is assumed to have a time-averaged value of 0.

Dual-wavelength Brillouin laser architecture

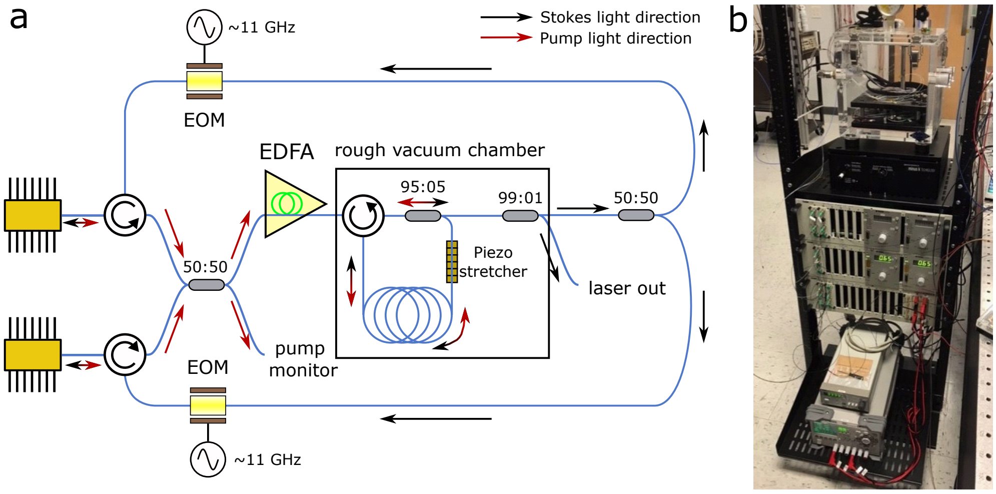

Fig. 1 Dual-wavelength Brillouin architecture. A schematic overview of the laser is shown in a. Black arrows indicate the direction of the Stokes light while red arrows indicate the direction of the pump light. A photograph of a rack-mounted iteration of the laser is shown in b.

Continuous, mode-hop-free operation

We continuously monitored the output of the dual-wavelength Brillouin source for over 48 hours using EO-comb frequency readout [4]. The results are plotted in Fig. 2. The output frequency drifts with room temperature, also plotted in Fig. 2 (black). Clear day-night cycles can be observed. While there are relatively fast frequency drifts, on the order of 5 minutes, frequency changes are less than 100 kHz from the average, far less than the $\sim$ 2.4 MHz FSR of the cavity indicating mode-hop-free operation over more than 2 days.

THz power and amplitude noise

In Fig.3a, we present a graph delineating the relationship between the radiated power and the measured photocurrent from a uni-traveling-carrier photodiode (UTC-PD). Since the UTC-PD is coupled to a millimeter-wave waveguide, it is noteworthy that the UTC-PD deployed for the 300 GHz measurements differs from the one utilized for the 600 and 700 GHz assessments. Likewise, two Schottky barrier diodes were used; one for the measurements at 300 GHz, and one for the measurements at 600 and 700 GHz. The specified responsivity for the 300 GHz photodiode is 0.24 A/W. For the UTC-PD at 600 GHz, the responsitivity is about 0.14 A/W.

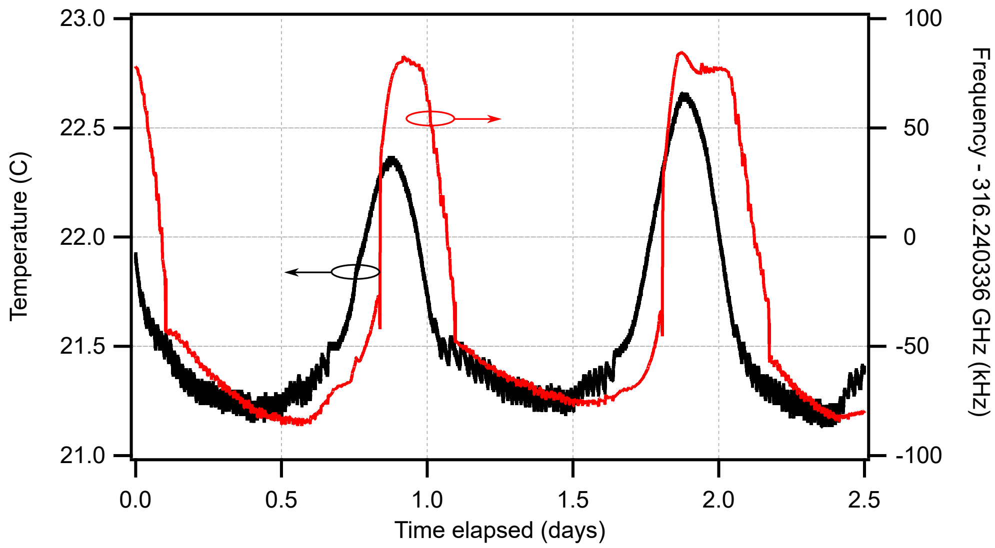

Fig. 2 Dual-wavelength Brillouin opto-THz output with time. The opto-THz frequency output of the dual-wavelength Brillouin is plotted in red. The frequency changes with room temperature, but does not mode hop over the 2.5 days of measurement time.

The UTC-PDs operating at 300 GHz and 600 GHz are interfaced with WR-3.4 and WR-1.5 rectangular metallic waveguides, respectively. These configurations are meticulously designed to ensure optimal functionality within their corresponding frequency bands of 300 GHz and 600 GHz. A broadband coupling circuit, monolithically integrated with the photodiode chip, facilitates the transition between the UTC-PD and the waveguide. The constructed module exhibits a 3-dB bandwidth of hundreds of GHz, indicative of its robust operational capacity across a substantial portion of the terahertz spectrum. Specifically, the photomixer's frequency span at 300 GHz covers 200 GHz to 400 GHz, while at 600 GHz, it extends from 450 GHz to 900 GHz.

To empirically demonstrate the impact of emitting lower power, we conducted measurements of the power spectral density of amplitude noise at two distinct terahertz frequencies: 300 GHz and 600 GHz, as depicted in Fig. 3b. The methodology involved a straightforward coupling of a single Schottky barrier diode, serving as an amplitude detector, with the UTC-PD. For the 300 GHz carrier, a white noise floor at -130 dB/Hz was observed, whereas the 600 GHz carrier displayed a noise floor at -110 dB/Hz. Additionally, flicker noise, characterized by a 1/f frequency dependence, was detected, which is postulated to originate from the Schottky barrier diode; however, this aspect was not explored within the scope of this study. Similarly, the potential saturation effects of the Schottky diode at 300 GHz, which could present a deceptively lower Relative Intensity Noise (RIN) in comparison to the 600 GHz scenario, were not investigated. Across all frequencies, the measured RIN of the radiated terahertz waves exceeded that of both Brillouin lines quantified in the optical domain

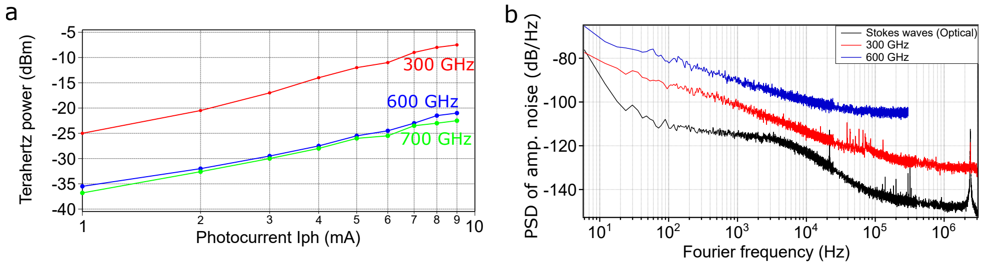

Fig. 3 UTC-PD power output and Brillouin RIN. a: Radiated THz power as a function of UTC-PD photocurrent. **b:** Power spectral density of the relative intensity/amplitude noise of the Brillouin opto-THz source measured after photomixing at 300 GHz (red), after photomixing at 600 GHz (blue), and in the optical domain (black).

Brillouin optical spectra

The optical spectrum of two separate dual-wavelength Brillouin systems, combined through a 50:50 coupler, is shown in Fig. 4. This configuration was used for phase noise measurements at 600 and 700 GHz, as detailed in the main text. When this spectrum undergoes photodetection, two terahertz waves, at 600 GHz and 600.1 GHz are emitted. These waves are then down-converted to baseband with the use of a Schottky diode.

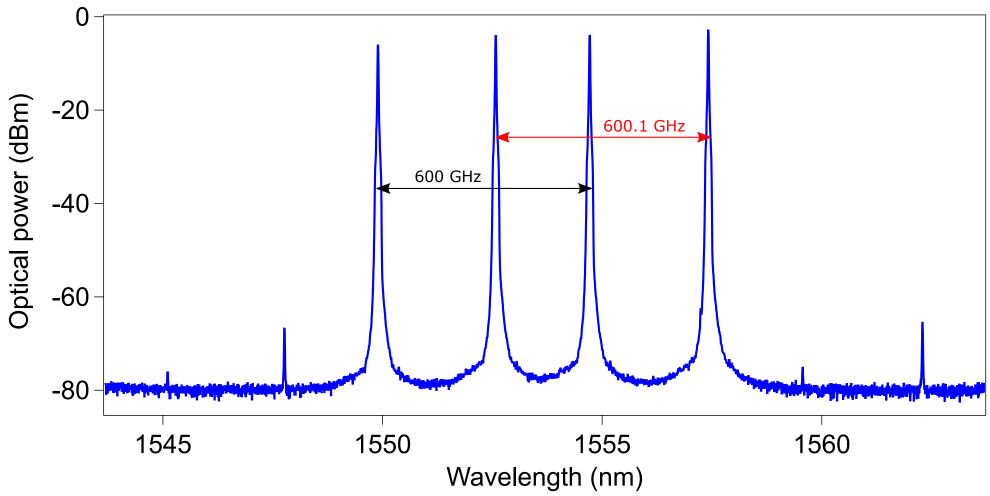

Fig. 4 Combined optical spectra of two Brillouin lasers. This configuration is used to measure the phase noise in the WR1.5 band. The optical signal to noise on each line is greater than 70 dB.

Measurement of 3 THz phase noise and limitations of TWDI

We conducted phase noise measurements at 3 THz using a two-wavelength delayed interferometer (TWDI) as shown in Fig. 5a. The result of this measurement is plotted in Fig. 5c.

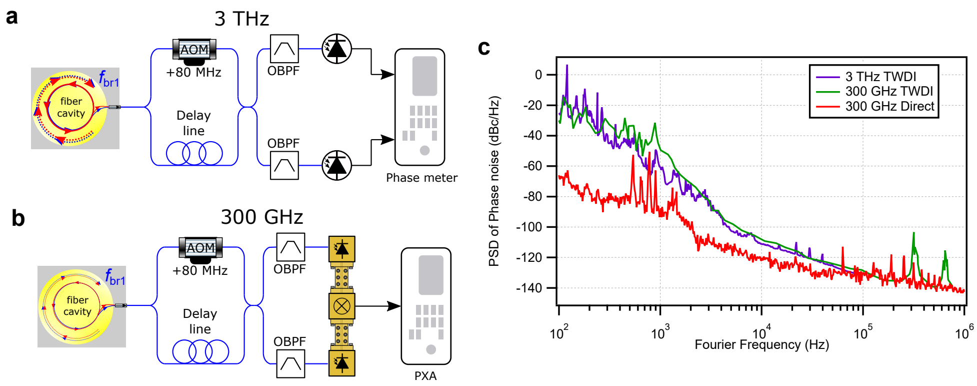

Fig. 5 Phase noise measurements at 3 THz and their limitations. Phase Noise Characterization at THz Frequencies. (a) illustrates the TWDI setup for 3 THz phase noise measurement, and (b) for 300 GHz, with the latter using UTC-PD's for wave radiation. (c) shows that similar phase noise results (purple for 3 THz and green for 300 GHz) suggest limitation by fiber noise in the delay line. The more accurate 300 GHz phase noise (red), as detailed in the main text, indicates that TWDI provides only an upper limit for phase noise, especially at 3 THz.

In order to assess the limitations of this measurement, we also characterized the phase noise of 300 GHz radiation using our TWDI. However, for 300 GHz measurements, the opto-THz wave was converted to THz using two separate UCT-PDs and subsequently mixed on a fundemental mixer, as shown in Fig. 5b.

The results of these experiments are summarized in Fig. 5c. Notably, the TWDI measurements for both 3 THz (illustrated in purple) and 300 GHz (shown in green) exhibit nearly identical phase noise profiles. This parallelism strongly implies that the phase noise is predominantly influenced by the fiber noise introduced by the delay line, as referenced in [5], and this phenomenon constrains the measurement accuracy at both tested frequencies—0.3 and 3 THz.

A more sensitive measurement of phase noise at 300 GHz, detailed within the main body of the text and duplicated here in Fig.5c (red line), corroborates that the limitations of the TWDI method affected our ability to accurately quantify phase noise at 300 GHz. When these observations are considered collectively, they lead to the conclusion that the TWDI methodology, as implemented in our experiments, is not sufficiently sensitive to ascertain the true phase noise at 3 THz. Instead, our findings represent an upper boundary of the phase noise, underscoring the need for enhanced measurement techniques to fully characterize the noise profile at this high frequency.

References

[1] Born, M., Wolf, E.: Principle of optics, cambridge university press. Cambridge (1999)

[2] Ishibashi, T., Ito, H.: Uni-traveling carrier photodiodes: Development and prospects. IEEE Journal of Selected Topics in Quantum Electronics **28**(2: Optical Detectors), 1–6 (2021)

[3] Quinlan, F.: The photodetection of ultrashort optical pulse trains for low noise microwave signal generation. arXiv preprint arXiv:2302.14786 (2023)

[4] Rolland, A., Loas, G., Brunel, M., Frein, L., Vallet, M., Alouini, M.: Non-linear optoelectronic phase-locked loop for stabilization of opto-millimeter waves: towards a narrow linewidth tunable thz source. Optics express **19**(19), 17944–17950 (2011)

[5] Kuse, N., Fermann, M.E.: A photonic frequency discriminator based on a two wavelength delayed self-heterodyne interferometer for low phase noise tunable micro/mm wave synthesis. Scientific Reports **8**(1), 13719 (2018) https://doi.org/10.1038/s41598-018-31712-y